ELSEVIER

Journal of Chromatography B, 755 (2001) 91–99

JOURNAL OF CHROMATOGRAPHY B

www.elsevier.com/locate/chromb

Use of non-covalent labeling in illustrating ligand binding to human serum albumin via affinity capillary electrophoresis with near-infrared laser induced fluorescence detection

John Sowell, Kimberly A. Agnew-Heard, J. Christian Mason, Charles Mama, Lucjan Strekowski, Gabor Patonay*

Department of Chemistry, University Plaza, Georgia State University, Atlanta, Georgia, GA 30303, USA

Received 16 August 2000; received in revised form 5 January 2001; accepted 5 January 2001

Abstract

This paper demonstrates the use of a near-infrared (NIR) dye as a non-covalent label for human serum albumin (HSA). The dye is a water soluble, heptamethine cyanine dye. The utility of the dye as a tracer illustrating the binding of various drugs to HSA is demonstrated via affinity capillary electrophoresis with near-infrared laser-induced fluorescence detection (ACE-NIR-LIF). Additionally, the factors affecting the separation of relevant species were investigated. The change in quantum yield of the dye upon complexation with HSA was calculated. Spectrophotometric measurements were conducted to study the stoichiometry of the dye albumin complex.

Keywords: Non-covalent labeling; Human serum albumin

1. Introduction

Affinity Capillary Electrophoresis is a technique which refers to the separation of compounds that engage in affinity interactions [1]. There are three main modes of ACE. The receptor-ligand mixture may be equilibrated offline [1]. The run buffer may contain either receptor or ligand [1]. Finally, receptor or ligand may be immobilized on the capillary [1]. The most common methods of detection via ACE are absorbance and laser-induced fluorescence (LIF). Detection by LIF offers several advantages over absorbance detection. One advantage is that the low background noise associated with LIF detection, results in improved sensitivity [2]. Another advantage of LIF detection is improved selectivity. Some analytes are not intrinsically fluorescent, making it necessary to label the analyte with a fluorescent tag. Since only the species of interest is labeled, unwanted background signals are potentially reduced [3]. Fluorescent labeling of analytes also allows molecules that lack native fluorescence to be detected via LIF.

Most LIF detection schemes use a fluorophore that is covalently attached to the species of interest, however, covalent labeling does have disadvantages. Derivitization reactions are time consuming. In addition, covalent derivitization requires rigorous control of the pH in order to maintain satisfactory labeling efficiency [3]. For example, a dye which has an

*Corresponding author. Tel.: +1-404-651-3856; fax: +1-404-651-1416.

E-mail address: cheggp@panther.gsu.edu (G. Patonay).

0378-4347/01/$ – see front matter
PII: S0378-4347(01)00035-4

isothiocyanato functionality that is reactive toward primary amines could be used to label proteins, however, the amine groups on the protein will only be deprotonated at high pH values. The high pH values necessary for the derivitization reaction to occur may not be tolerable when working with biological samples. Another disadvantage of covalent labeling is that analyte molecules often have differing numbers of dyes attached to them, leading to band broadening [4]. Furthermore, purification steps are often necessary to remove excess, unreacted dye [5]. Because of these disadvantages, non-covalent labeling schemes are advantageous in that they are significantly faster than traditional covalent labeling, control of pH may not be as critical, and, if the stoichiometry of the labeling reaction is known, purification steps may not be necessary.

A source of interference often encountered when using visible fluorescent dyes is background fluorescence exhibited by the sample matrix. The use of NIR dyes as fluorescent labels eliminates unwanted fluorescence signals, since very few molecules exhibit intrinsic fluorescence in the NIR region of the spectrum (~670–1000 nm). Thus, the NIR region is especially well suited for bioanalytical applications where autofluorescence of the sample matrix is a problem [6]. NIR dyes generally have good molar adsorptivities (ϵ~150 000–200 000). The quantum yields of NIR dyes, typically in the range of 0.05–0.5, increase upon complexation [7,8]. Another advantage of NIR dyes is that scatter noise (Raman and Rayleigh) is reduced since it is related to the wavelength of detection by $1/\lambda^4$ [6]. In addition, LIF detection in the NIR region of the spectrum allows for the use of solid state components. Diode lasers, having the advantages of long operating lifetimes, compactness, and low cost, may be used as excitation sources [6]. Avalanche photodiodes (APD) may be used for detection. APD's have long operating lifetimes and low noise characteristics [6]. When used in the NIR, quantum efficiencies of 80% are typical of APD's.

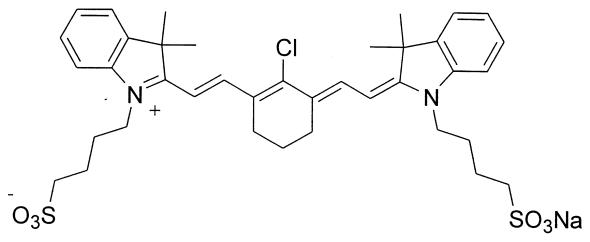

Fig. 1. Structure of heptamethine cyanine dye used in experiments.

The use of diode lasers in CE LIF detection schemes has been previously demonstrated [6,9,10]. Furthermore, Colyer [3] and co-workers have used the near-infrared dye indocyanine green to non-covalently label human serum albumin. In this manuscript, a NIR dye (Fig. 1), synthesized in our laboratories was used to non-covalently label HSA. The dye is then used as a tracer illustrating the binding of various drugs to HSA. Drug binding is demonstrated in two separate ways, competitive and noncompetitive, with respect to dye. The stoichiometry of the dye–protein complex is investigated. The change in the quantum yield of the dye, upon complexation with albumin, is calculated. Parameters affecting the separation of relevant species were also investigated.

Human serum albumin is one of the most abundant proteins in the human body. Albumin is probably best known for its ability to bind ligands of diverse chemical and physical characteristics [11]. Drug-interactions with albumin influence the drug's toxicity, activity, excretion, and metabolism [11]. It is therefore of interest to develop techniques that can characterize the nature of drug–albumin interactions. Techniques that have been used to study ligand–albumin interactions include equilibrium dialysis [12], flow injection [13], circular dichroism [14–16], fluorescence titration [16], crystallography [17,18], and affinity capillary electrophoresis [19–24]. While these techniques have their advantages, most are slow, labor intensive, susceptible to matrix effects, and use large amounts of reagent. We have developed a CE based technique that allows one to determine a compounds' potential to interact with albumin. The technique is fast, sensitive, and is less susceptible to matrix interferences since detection is in the NIR.

2. Experimental

2.1. Reagents

Human serum albumin, boric acid, warfarin, sodium dibasic phosphate, phosphoric acid, ibuprofen,

fenoprofen, ketoprofen, quinidine, cholrpromazine, naproxen, sulfisoxazole, imipramine, stearic acid, and sodium hydroxide were obtained from Sigma (St. Louis, MO, USA). Borate buffer, 200 m*M*, pH 9.0, was prepared by dissolving the appropriate amount of boric acid in nanopure grade water (Barnstead model D4571 ultrapure water system). The pH was adjusted by addition of 0.5 *N* sodium hydroxide. Phosphate buffer, 100 m*M*, pH 7.2, was prepared by dissolving the appropriate amount of sodium phosphate in water. The pH was adjusted by addition of phosphoric acid. Protein, dye, and drug solutions were made by dissolving the appropriate amounts of each reagent into 100 m*M*, pH 7.2, phosphate buffer. All solutions were stored in the dark at 4°C prior to use.

2.2. Synthesis of NIR dye

Cyanine dye was synthesized by the published procedure [25] with slight modification given below.

2.2.1. Sodium 4-[2-[4-chloro-7-[3,3-dimethyl-1-(4-sulfonatobutyl)indolin-2-ylidene]-3,5-(propane- 1,3-diyl)-1,3,5-heptatrien-1-yI]-3,3-dimethyl-3H-indolio]butanesulfonate [25]

4-(2,3,3-Trimethyl-3*H*-indolio)butanesulfonate [25] (626 mg, 2 mmol), *N*-[5-anilino-3-chloro-2,4-(propane-1,3-diyl)-2,4-pentadien-1-ylidene]anilinium chloride [26] (359 mg, 0.96 mmol) and anhydrous sodium acetate (164 mg, 2 mmol) were heated under reflux in absolute ethanol under a nitrogen atmosphere for 5 h. The solvent was then removed in vacuo and purified by column chromatography on silica gel using a gradient of diethyl ether: acetone:methanol. The solvent was then removed under vacuum to give a dark red solid; yield 80% (576.5 mg, 0.77 mmol); spectral data have been reported previously [25].

2.3. Apparatus

All CE experiments used a modified P/ACE 5000 capillary electrophoresis instrument (Beckman Instruments, Inc., Fullerton, CA). The instrument was interfaced with a proprietary microscope and laser assembly. The laser assembly consists of a diode laser emitting at 787 nm, modulated with a 50% duty cycle. The diode laser is focused directly onto a fiber optic cable. The arrangement gives 4 mW of power at the capillary interface. Detection is accomplished via a Peltier cooled, three stage avalanche photodiode. Three bandpass filters (820±10 nm) are used in order to minimize background noise. The APD signal is demodulated by a lock in amplifier. The signal is filtered before it arrives at a Beckman 406 A/D converter. The signal is then collected by a personal computer. A more detailed description of the instrument is available elsewhere [27]. Fluorescence measurements were made on an ISS K2 (ISS, Champaign, IL) multiphase fluorometer. Absorbance measurements were performed on a Perkin-Elmer Lamba 20 (Perkin-Elmer, Norwalk, CT) UV/VIS/NIR spectrophotometer.

2.4. Capillary electrophoresis

All experiments were performed at 23°C. The primary electrophoresis run buffer was 200 m*M* borate buffer adjusted to a pH of 9.0. All buffers were filtered and sonicated prior to use. All separations were performed using fused-silica capillaries with a polyimide coating (Polymicro Technology, Phoenix, AZ). Total capillary length was 57 cm, with an injection to detection length of 50 cm. The internal diameter of the capillary was 50 μm. At the beginning of each day, the capillary was rinsed with 1 *N* sodium hydroxide for 30 min, followed by 15 min rinses with water and run buffer, respectively. All samples were introduced by pressure injection (5 s at 0.5 p.s.i.). Voltage was applied over a 30 s ramp time. Following each run, the capillary was rinsed with run buffer for 5 min.

2.5. Non-covalent labeling procedure

The non-covalent labeling of HSA was carried out by mixing aliquots of the protein and dye solutions. The mixture was then vortexed for 30 s. The desired drug/ligand was then added to the mixture and the solution was vortexed again for 30 s. Prior to use, the mixture was diluted with phosphate buffer, 100 m*M*, pH 7.2, to the desired concentration.

3. Results and discussion

3.1. Utility of dye as a non-covalent label

The use of non-covalent labeling offers several advantages over conventional, covalent labeling schemes, as previously mentioned. The utility of the dye as a non-covalent label was investigated. The electropherograms of fixed dye concentration with increasing HSA concentration is illustrated in Fig. 2 A–D. As the concentration of protein is increased, with respect to a fixed dye concentration, the labeled protein peak increases while the free dye peak decreases, suggesting that the dye is suitable as a non-covalent label for HSA. The peak associated with dye-labeled protein is fairly broad. Furthermore, peak splitting was sometimes observed with the protein peak suggesting that there may be multiple dye–protein species present. Dovichi and co-workers [4] have done work demonstrating that excessive peak width such as this is indeed due to the partial resolution of multiple species.

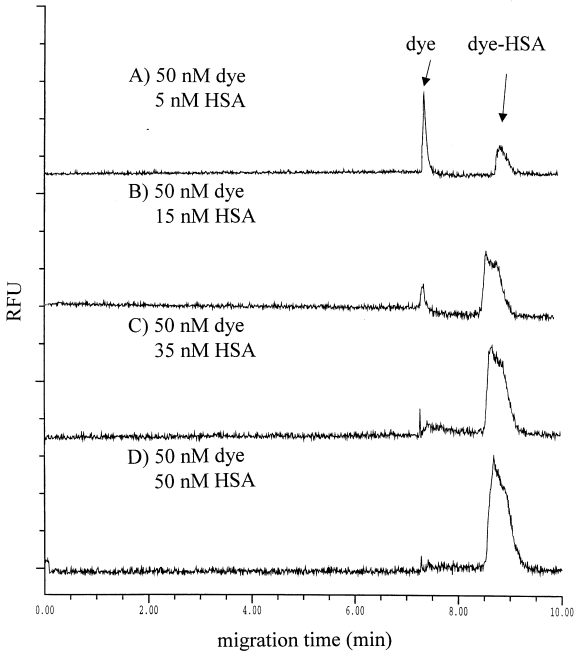

Fig. 2. Comparison of electropherograms of fixed dye concentration with increasing protein concentration. (A), 50 n*M* dye and 5 n*M* HSA; (B), 50 n*M* dye and 15 n*M* HSA; (C), 50 n*M* dye and 35 n*M* HSA; (D), 50 n*M* dye and 50 n*M* HSA. Conditions; capillary length 57 cm; internal diameter, 50 μm; applied voltage, 20 kV; 200 m*M* borate, pH 9.0; 5 sec injection at 0.5 p.s.i.

Upon inspection of Fig. 2, it may be seen that the total area of the peaks is not the same. Previously, it was shown that the fluorescence intensity of cyanine dyes increases upon complexation, due to shielding effects [7,8]. A similar trend was observed in this experiment (Fig. 2). The change in quantum yield of the dye upon complexation was calculated by taking the ratio of labeled protein peak area to the area corresponding to disappearance of free dye. For example, if the change in the free dye peak area upon addition of protein was 2, and the peak area of the corresponding labeled protein peak was 10, then the change in the quantum yield is 5. It was necessary to correct for peak area differences due to differences in migration time, since analytes migrating at different rates will be in the detection window for different amounts of time. It was found that the quantum yield of the dye increased by a factor of ten upon complexation with HSA.

3.2. Noncompetitive binding of warfarin to albumin

It was of interest to determine if the dye could be used as a tracer to monitor drug binding to HSA. Warfarin is an anticoagulant known to bind to human serum albumin at site I [11]. It was found that the dye could be used as a tracer illustrating the binding of warfarin to NSA, as seen in Fig. 3. Fig. 3A is free protein and dye labeled protein. The addition of warfarin results in the appearance of another peak, presumably due to the binding of warfarin to dye-labeled HSA (Fig. 3B,C). Low concentrations of warfarin resulted in a peak that could not be baseline resolved. However, higher concentrations of warfarin did give a baseline resolved peak.

3.3. Optimization of separation conditions

It was necessary to determine the separation conditions which provided the best resolution between free dye, dye–protein, and dye–protein–warfarin. The concentration of borate buffers, pH 9.0, was varied from 25 to 200 m*M*. Results showed that increasing the ionic strength improved resolution between free dye, dye–protein, and dye–protein–

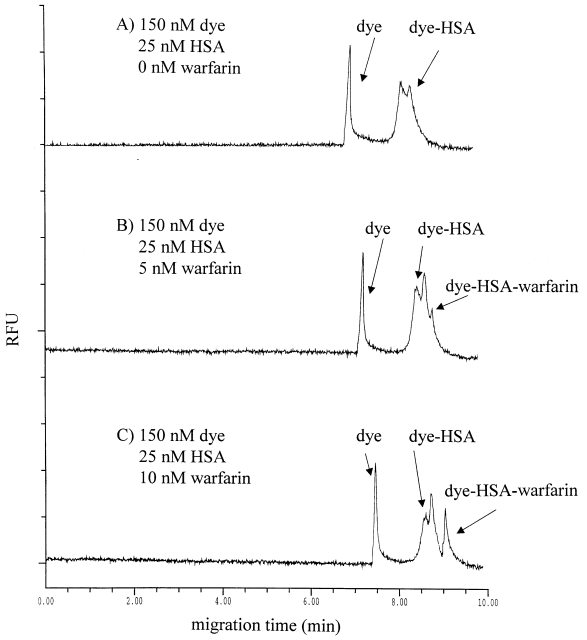

Fig. 3. Electropherograms illustrating the effect of adding warfarin. (A), 150 n*M* dye and 25 n*M* HSA; (B), 150 n*M* dye, 25 n*M* HSA, and 5 n*M* warfarin; (C), 150 u*M* dye, 25 n*M* HSA, and 10 n*M* warfarin. Conditions as in Fig. 2.

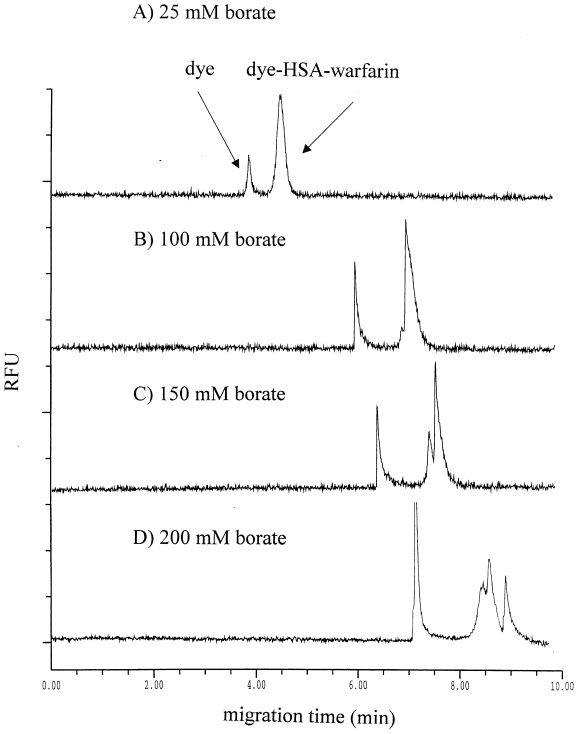

Fig. 4. Comparison of electropherograms of noncompetitive binding of warfarin to HSA at different ionic strengths; 150 n*M* dye, 25 n*M* HSA, and 10 n*M* warfarin. (A), 25 m*M* borate; (B,) 100 m*M* borate; (C), 150 m*M* borate; (D), 200 m*M* borate. Conditions as in Fig. 2.

warfarin (Fig. 4). While it was possible to resolve free dye from dye-labeled protein with 25 m*M* borate buffer, the peak corresponding to protein bound warfarin was only resolved at 200 m*M* borate buffer.

Protein separations performed using capillary electrophoresis are often complicated due to adsorption effects between the capillary wall and the protein [28]. Although coated capillaries may be used to minimize these effects, it is often more convenient to use standard fused-silica capillaries [3]. The use of high pH buffers may minimize protein adsorption effects if the buffer pH is greater than the isoelectric point of the protein. It was found that a pH 9.0 borate buffer resulted in the baseline resolution of free dye, dye–HSA, and dye–HSA–warfarin (Fig. 5). Buffers of pH 8.0, 8.5, and 9.5 were unable to adequately resolve free dye, dye–HSA, and dye–HSA–warfarin (Fig. 5).

The free dye, dye–HSA, and dye–HSA–warfarin mixture was separated in 200 m*M* borate buffer, pH 9.0, at various applied voltages. All species present were resolved at each of the voltages (Fig. 6). However, an applied voltage of 20 kV gave the best results, with respect to peak intensity. At 25 kV and 15 kV, the peak intensities of the dye–HSA–warfarin complex decreased with respect to the complexes' peak intensity at 20 kV (Fig. 6).

3.4. Competitive binding of additional ligands

While warfarin was the only compound which resulted in the appearance of an additional peak in the electropherograms, the binding of a number of other compounds was demonstrated through competitive binding. There exist two ways in which the dye may be used to illustrate ligand binding to HSA. The noncompetitive based method has already been shown via warfarin. However, the dye and ligand may bind at the same location on HSA. If this is the case, the ligand may displace some of the dye which is attached to the protein. Fig. 7A is an elec-

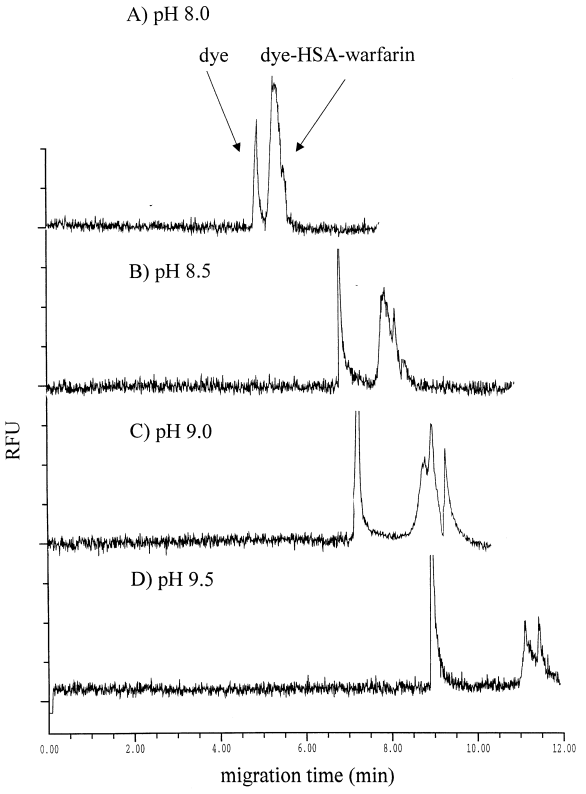

Fig. 5. Comparison of electropherograms of noncompetitive binding of warfarin to HSA at different pH values. (A), pH 8.0; (B), pH 8.5; (C), pH 9.0; (D), pH 9.5. Conditions as in Fig. 2.

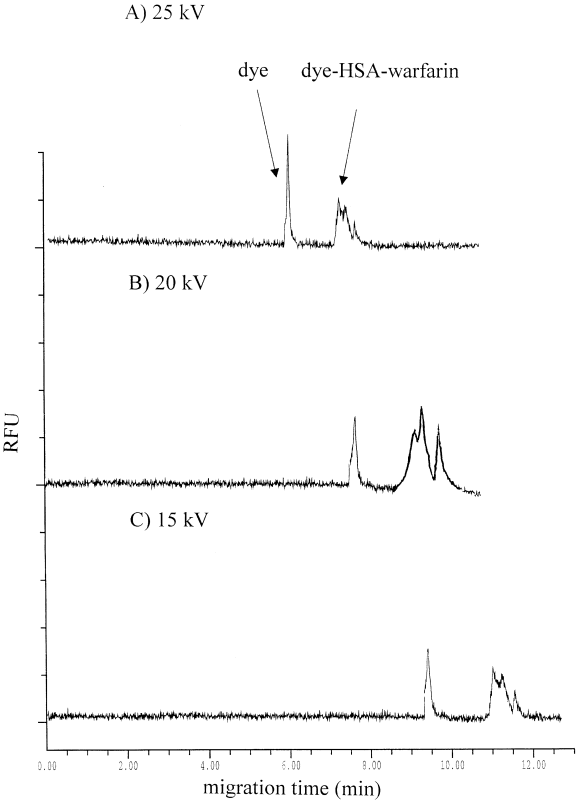

Fig. 6. Comparison of electropherograms of noncompetitive binding of warfarin to HSA at different applied voltages. (A), 25 kV; (B), 20 kV; (C), 15 kV. Conditions as in Fig. 2.

tropherogram of free dye and dye-labeled protein. The electropherograms in Fig. 7B–D have the same concentrations of dye and protein as in Fig. 7A, however, stearic acid (Fig. 7B), naproxen (Fig. 7C), and quinidine (Fig. 7D) have been added. It is known that stearic acid, quinidine, and naproxen all bind to HSA at site II [11]. It can be seen from the electropherograms in Fig. 7, that when these ligands are added, the peak corresponding to labeled HSA decreases and the free dye peak increases. This suggests that a competitive type interaction exists between the dye and the ligands. In order to confirm that the observed data was not due to dissociation of the dye–protein complex, an equilibrated mixture of dye and HSA was repeatedly injected over 2 h. No significant degradation in the dye–HSA peak was observed.

It appears that the degree of dye displacement by ligand is directly correlated to the ligands' association constant for HSA. Stearic acid, having the highest association constant of the ligands shown, $6.9 \cdot 10^8$ *M* [11], displaces more dye than naproxen, whose association constant with HSA is $1.2 \cdot 10^6$ *M* [11]. Along those same lines, naproxen displaces more dye than quinidine, whose association constant is $1.6 \cdot 10^3$ *M* [11]. While the data is not shown, this competitive type binding was observed with ibuprofen, fenoprofen and ketoprofen.

3.5. Stoichiometry of NIR dye–HSA

Cyanine dyes may bind with proteins via hydrophobic [29] or through Coulombic interactions [28]. It is most likely that multiple dye–HSA complexes exist. Despite this, a number of techniques were used

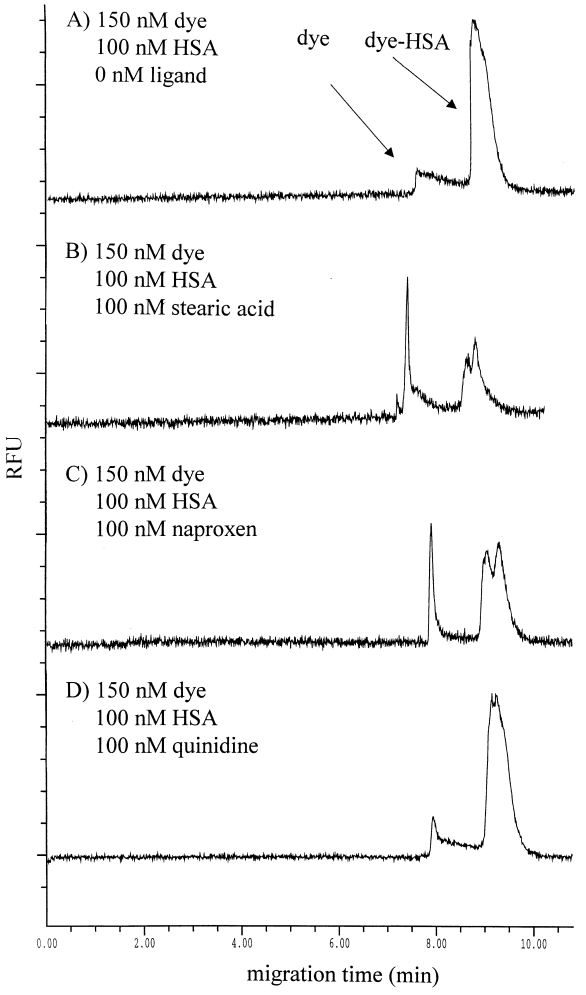

Fig. 7. Comparison of electropherograms illustrating the competitive binding of stearic acid, naproxen, and quinidine. (A), 150 n*M* dye and 100 n*M* HSA; (B), 150 n*M* dye, 100 n*M* HSA, and 100 n*M* stearic acid; (C), 150 n*M* dye, 100 n*M* HSA, and 100 n*M* naproxen; (D), 150 n*M* dye, 100 n*M* HSA, and 100 n*M* quinidine. Conditions as in Fig. 2.

in order to gain some insight into the stoichiometry of the dye–HSA complex.

Saturable binding curves, using both fluorescence and absorbance, were constructed. The fluorescence binding curve (Fig. 8), shows change in fluorescence intensity of a fixed concentration of dye, $5{\cdot}10^{-7}$ *M*, relative to increasing concentrations of HSA. Since the fluorescence intensity of the dye increases upon complexation with HSA, it would be expected that the fluorescence intensity would level off at the point

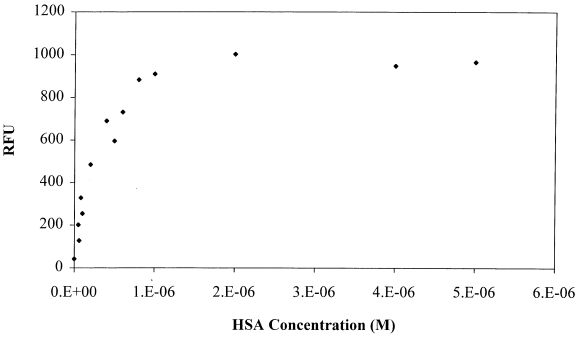

Fig. 8. Fluorescence binding curve: change in fluorescence intensity as a function of increasing HSA concentration. Dye concentration was fixed at $5{\cdot}10^{-7}$ *M*. Excitation was at 780 nm.

where all of the dye is complexed to protein. While a distinct plateau is not observed, a leveling off of the fluorescence intensity occurs at a HSA concentration of $\sim 7{\cdot}10^{-7}$ *M* (Fig. 8).

The point of maximum absorbance for the dye shifts upon complexation. The wavelength used in the absorbance binding curve corresponds to the λ_{max} of dye complexed with HSA, consequently free dye absorbance is minimized. The absorbance spectrum of a fixed concentration of dye, $5{\cdot}10^{-6}$ *M*, relative to increasing concentrations of HSA is shown in Fig. 9. A leveling off of the absorbance is observed at a HSA concentration of $5{\cdot}10^{-6}$ M.

A definitive stoichiometry of the complex could not be determined from the data provided by the absorbance and fluorescence binding curves. Consequently, a Job's plot was used to determine the

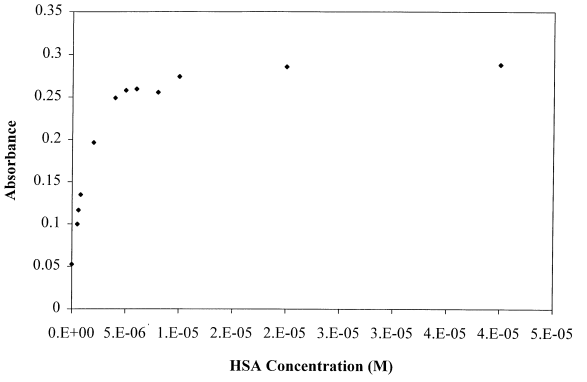

Fig. 9. Absorbance binding curve: change in absorbance as a function of HSA concentration. Dye concentration was fixed at $5{\cdot}10^{-6}$ *M*. Absorbance was measured at 806 nm.

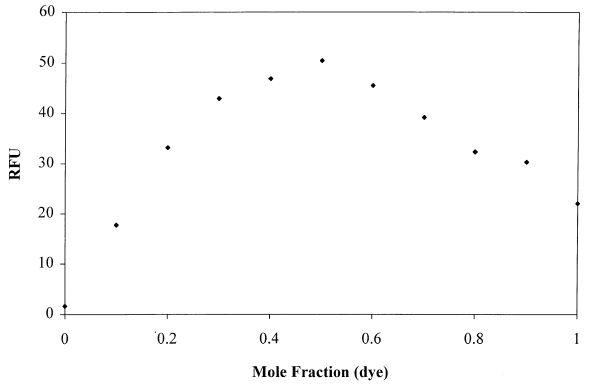

Fig. 10. Job's plot for calculating the primary dye–HSA species. The total concentration of dye and HSA was fixed while the mole fraction of dye was varied. Excitation was at 780 nm.

primary form of the dye–HSA complex (Fig. 10). The total concentration of dye and HSA remained constant, however the mole fraction of the dye was varied. The maxima of the Job's plot represents the primary form of the complex present. From the Job's plot, a 1:1 stoichiometry for the primary species of the complex was determined. This stoichiometry is in agreement with the binding curve data obtained in Figs. 8,9. Furthermore, in Fig. 2D, it appears that nearly all the dye is bound to HSA, when dye and HSA are present in a 1:1 ratio. It should be noted that this is only the predominant form of the complex present. It is likely that multiple stoichiometries of the complex exist.

4. Conclusion

In this work we have developed a fast, sensitive, qualitative method to test for a compound's potential to bind with HSA. Furthermore, based on the type of interactions exhibited by the ligand, some information on the location of the ligand binding site may be obtained. Based on the competitive interactions observed, it appears that the dye binds to subdomain IIIA, commonly referred to as site II, due to the fact that competitive interactions were not observed with site I binding drugs. The utility of the NIR dye used in the experiments as a non-covalent label for HSA has been demonstrated. As has been shown, non-covalent labeling schemes offer multiple advantages over traditional labeling techniques, i.e., minimal sample preparation and purification. The predominant form of the dye–HSA complex was determined to have a 1:1 stoichiometry. Furthermore, it has been demonstrated that the dye may be used as a probe to monitor ligand binding to HSA by two different methods. A noncompetitive format for monitoring ligand binding to HSA was developed using warfarin. It should be noted that warfarin is the only compound tested which exhibited this type of binding. A competitive based method, in which the dye and ligand compete for the same binding site on HSA, for monitoring ligand binding with HSA was also developed. Since albumin is known to bind a large variety of compounds, it is of potential interest to develop methodology which allows one to determine if a ligand will interact with albumin.

Acknowledgements

John Sowell is a recipient of the Solvay Pharmaceuticals Graduate Fellowship in Analytical Chemistry.

References

[1] N.H.H. Heegaard, S. Nilsson, N.A. Guzman, J. Chromatogr. B 715 (1998) 29.
[2] S.L. Pentoney Jr., J.V. Sweedler, in: J.P. Landers (Ed.), Handbook of Capillary Electrophoresis, 2nd ed, CRC Press, Boca Raton, FL, 1997, p. 379, Chapter 12, and references contained therein.
[3] E.D. Moody, P.J. Viskari, C.L. Colyer, J. Chromatogr. B 729 (1999) 55.
[4] D.B. Craig, N.J. Dovichi, Anal. Chem. 70 (1998) 2493.
[5] N.M. Schultz, L. Huang, R.T. Kennedy, Anal. Chem. 67 (1995) 924.
[6] M.J. Baars, G. Patonay, Anal. Chem. 71 (1999) 667.
[7] D. Andrew-Wilbeforce, G. Patonay, Spectrochim. Acta 46A (1990) 1153.
[8] M.D. Antoine, S. Devanathan, G. Patonay, Spectrochim. Acta 47A (1991) 501.
[9] D.C. Williams, S.A. Soper, Anal. Chem. 67 (1995) 3427.
[10] B.L. Legendre Jr., D.L. Moberg, D.C. Williams, S.A. Soper, J. Chromatogr. A 779 (1997) 185.
[11] T. Peters, in: All About Albumin: Biochemistry, Genetics, And Medical Applications, Academic Press, San Diego, CA, 1996, p. 76, Chapter 3 and references contained therein.
[12] F. Lagrange, F. Penhourcq, M. Matoga, B. Bannwarth, J. Pharm. Biomed. Anal. 23 (5) (2000) 793.

[13] M.E. Georgiuo, C.A. Georgiou, M.A. Koupparis, Anal. Chem. 71 (1999) 2541.
[14] N. Okabe, N. Mannabe, R. Tokuoka, K. Tomita, J. Biochem. 77 (1975) 181.
[15] M. Zandomeneghi, Chirality 7 (1995) 446.
[16] M. Dockal, M. Chang, D.C. Carter, F. Ruker, Protein Sci. 9 (2000) 1455.
[17] A.A. Bhattacharya, S. Curry, N.P. Franks, J. Biol. Chem. (2000) [epub ahead of print].
[18] A.A. Bhattacharya, T. Grune, S. Curry, J. Mol. Biol. 303 (2000) 721.
[19] J. Yang, D.S. Hage, Anal. Chem. 66 (1994) 2719.
[20] Y. Ding, X. Zhu, B. Lin, Electrophoresis 20 (1999) 1890.
[21] V. Andrisano, R. Gotti, V. Cavrini, V. Tumiatti, G. Felix, I.W. Wainer, J. Chromatogr. A 803 (1998) 189.
[22] Y.H. Chu, L.Z. Avila, H.A. Biebuyck, G.M. Whitesides, J. Med. Chem. 35 (1992) 2915.
[23] P. Sun, A. Hoops, R.A. Hartwick, J. Chromatogr. B 661 (1994) 335.
[24] Y.H. Chu, W.J. Lees, A. Stassinopoulos, C.T. Walsh, Biochemistry 33 (1994) 10616.
[25] M. Lipowska, G. Patonay, L. Strekowski, Synth. Comm. 23 (1993) 3807.
[26] S.M. Makin, L.I. Boiko, O.A. Shavrygina, Org. Khim. 13 (1977) 1189.
[27] M.J. Baars, G. Patonay, Appl. Spectrosc. 52 (1999) 1619.
[28] B.L. Legendre, S.A. Soper, Appl. Spectrosc. 50 (1996) 1196.
[29] K. Sauda, T. Imasaka, N. Ishibashi, Anal. Chem. 58 (1986) 2649.